

UNCLASSIFIED

AD NUMBER
AD852308
NEW LIMITATION CHANGE
TO Approved for public release, distribution unlimited
FROM Distribution authorized to U.S. Gov't. agencies and their contractors; Critical Technology; MAY 1969. Other requests shall be referred to Air Force Weapons Laboratory, Attn: WLDC, Kirtland AFB, NM.
AUTHORITY
afwl ltr, 30 nov 1971

THIS PAGE IS UNCLASSIFIED

AFWL-TR-68-144

AFWL-TR-
68-144

**PRESSURE PULSE MOVING WITH CONSTANT
VELOCITY ON THE SURFACE OF A LAYERED
MATERIAL (LOCKING-ELASTIC LAYER-
SUBSEISMIC HALF-SPACE)**

Guy Bertrand Melvin L. Baron

With the cooperation of Hans H. Bleich

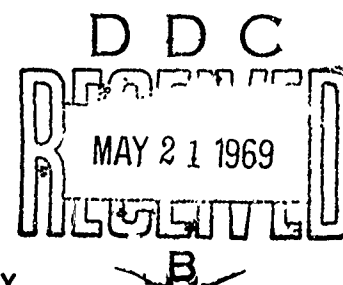
Paul Weidlinger & Associates

New York, New York

Contract No. F29601-67-C-0091

TECHNICAL REPORT NO. AFWL-TR-68-144

May 1969



AIR FORCE WEAPONS LABORATORY

Air Force Systems Command

Kirtland Air Force Base

New Mexico

This document is subject to special export controls and each transmittal to foreign governments or foreign nationals may be made only with prior approval of AFWL (WLDC), Kirtland AFB, NM, 87117.

AD852308



AIR FORCE WEAPONS LABORATORY
Air Force Systems Command
Kirtland Air Force Base
New Mexico

When U. S. Government drawings, specifications, or other data are used for any purpose other than a definitely related Government procurement operation, the Government thereby incurs no responsibility nor any obligation whatsoever, and the fact that the Government may have formulated, furnished, or in any way supplied the said drawings, specifications, or other data, is not to be regarded by implication or otherwise, as in any manner licensing the holder or any other person or corporation, or conveying any rights or permission to manufacture, use, or sell any patented invention that may in any way be related thereto.

This report is made available for study with the understanding that proprietary interests in and relating thereto will not be impaired. In case of apparent conflict or any other questions between the Government's rights and those of others, notify the Judge Advocate, Air Force Systems Command, Andrews Air Force Base, Washington, D. C. 20331.

DO NOT RETURN THIS COPY. RETAIN OR DESTROY.

ADDITION FOR	
CRFTI	WHITE SECTION <input type="checkbox"/>
DDC	BUFF SECTION <input checked="" type="checkbox"/>
UNANNOUNCED	<input type="checkbox"/>
JUSTIFICATION	
BY	
DISTRIBUTION/SECURITY CLASS	
EISE	AVAIL. and/or SPECIAL
2	

PRESSURE PULSE MOVING WITH CONSTANT VELOCITY
ON THE SURFACE OF A LAYERED MATERIAL
[LOCKING-ELASTIC LAYER - SUBSEISMIC HALF-SPACE]

Guy Bertrand Melvin L. Baron
With the cooperation of Hans H. Bleich

Paul Weidlinger & Associates
New York, New York
Contract No. F29601-67-C-0091

TECHNICAL REPORT NO. AFWL-TR-68-144

This document is subject to special export controls and each transmittal to foreign governments or foreign nationals may be made only with prior approval of AFWL (WLDC), Kirtland AFB, NM, 87117. Distribution is limited because of the technology discussed in the report.

FOREWORD

This report was prepared by Paul Weidlinger, Consulting Engineer, New York, New York, under Contract F29601-67-C-0091.

The research was performed under Program Element 61102H, Project 5710, Subtask SB144, and was funded by the Defense Atomic Support Agency (DASA).

Inclusive dates of research were January 1968 to November 1968. The report was submitted 14 March 1969 by the Air Force Weapons Laboratory Project Officer, Dr. Henry F. Cooper, Jr. (WLDC).

Information in this report is embargoed under the U.S. Export Control Act of 1949, administered by the Department of Commerce. This report may be released by departments or agencies of the U.S. Government to departments or agencies of foreign governments with which the United States has defense treaty commitments, subject to approval of AFWL (WLDC).

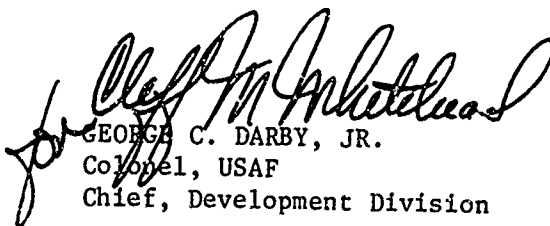
This technical report has been reviewed and is approved.



HENRY F. COOPER, JR.
Project Officer



CLIFF M. WHITEHEAD
Colonel, USAF
Chief, Civil Engineering Branch



GEORGE C. DARBY, JR.
Colonel, USAF
Chief, Development Division

ABSTRACT

(Distribution Limitation Statement No. 2)

The response of a layered half-space to a progressing normal surface pressure is evaluated. The half-space consists of a single layer of a locking material that acts elastically after compaction, and an underlying elastic material. The surface pressure moves with a constant velocity V , which is subseismic with respect to the speed of wave propagation in both the upper layer after compaction and the underlying half-space. It is assumed that a steady-state exists with respect to a coordinate axis attached to the moving load.

The essentially subseismic layer - subseismic half-space geometry leads to an elliptic problem that is solved by a finite difference iterative technique. A computer program for evaluating stresses and velocities at points in the medium is available and results are presented for a typical configuration of interest.

CONTENTS

<u>Section</u>	<u>Page</u>
I Introduction.	1
II Formulation of the Problem.	10
III Method of Solution.	17
1. Boundary Conditions at the Compaction Front.	22
2. Boundary Conditions on the Surface $z=0$ and on the Interface $z=H$ (Interface ahead of the Shock Front)	23
3. Continuity Conditions on the Interface behind the Compaction Front ($z=H$, $\xi > 0$)	24
4. Special Case for Point which is both on the Surface $z=0$ and the Compaction Front, Fig. 12.	25
5. Approximate Boundary Conditions at Large $ \xi $ and z , Figs. 6 and 7	28
6. Iterative Method for the Solution of the System of Linear Algebraic Equations using the Over- and Underrelaxation Technique.	30
7. Finite Difference Stress - Displacement Relations.	31
IV Numerical Results and Discussion.	33
References.	41
Distribution.	43

LIST OF ILLUSTRATIONS

<u>Figure</u>		<u>Page</u>
1	Loading Conditions	2
2	Approximation of Material by Locking-Elastic Model	2
3	Superseismic Layer - Subseismic Half-Space Geometry of Ref. [2]	5
4	Geometry of Present Problem	5
5	Approximate Geometry for Present Problem	7
6	Boundary Conditions at Large $ \xi $ and z	7
7	Boundary Conditions in Half-Space for Large $ \xi $ and z	8
8a	Plane Approximation for Compaction Front in Layer	8
8b	Boundary Conditions on Compaction Front	8
9	Finite Difference Grid and Axis Geometry for Numerical Solution	18
10	Finite Difference Grid	20
11	Displacement Resolution on Compaction Front	20
12	Special Case for Point Q	26
13	Vertical Stress σ_{zz} versus ξ in the Upper Layer	35
14	Horizontal Stress $\sigma_{\xi\xi}$ versus ξ in the Upper Layer	36
15	Shear Stress $\sigma_{\xi z}$ versus ξ in the Upper Layer	37
16	Vertical Stress σ_{zz} versus ξ in the Half-Space	38
17	Horizontal Stress $\sigma_{\xi\xi}$ versus ξ in the Half-Space	39
18	Shear Stress $\sigma_{\xi z}$ versus ξ in the Half-Space	40

LIST OF SYMBOLS

c_{P1}, c_{P2}	Dilatational wave speeds in regions 1 and 2.
c_{S1}, c_{S2}	Equivoluminal wave speeds in regions 1 and 2.
G_1, G_2	Shear modulus in regions 1 and 2.
H	Depth of layer.
i, j	Finite difference indices, Figs. 9 and 10.
h_r, h_ℓ	Pivotal point spacing of finite difference grid in ξ direction.
h_a, h_b	Pivotal point spacing of finite difference grid in z direction.
$M_L = V/c_S$	Cole-Huth Mach numbers.
$M_T = V/c_P$	Cole-Huth Mach numbers.
M_P, M_S	Mach numbers for dilatational and equivoluminal waves.
P_0	Magnitude of applied surface pressure.
t	Time.
u, v	Horizontal and vertical displacement coefficients.
$U(\xi)$	Heaviside unit step function.
$u^{(n)}, u^{(n+1)}$ $v^{(n)}, v^{(n+1)}$	Displacement components from the n^{th} and $n+1$ iteration, respectively.
V	Speed of moving surface load.
V_{cr}	Critical speed of moving surface load, associated with loading media, Eq. (25).
x	Horizontal coordinate in fixed Cartesian system.
z	Vertical coordinate in fixed Cartesian system.

α	Decay constant in loading function.
β	Angle of inclination of compaction front in locking material layer.
β_{cr}	Critical value of β , see Eq. (27).
ε_c	Critical strain for locking material, see Fig. 2.
λ_1, μ_1	Lamé elastic constants for layer (region 1).
λ_2, μ_2	Lamé elastic constants for half-space (region 2).
ν_1, ν_2	Poisson's ratio for regions 1 and 2.
$\xi = x + Vt$	Horizontal coordinate in moving Cartesian coordinate system.
ρ_1, ρ_2	Densities in regions 1 and 2.
$\sigma_{xx}, \sigma_{zz}, \sigma_{zx}$	Horizontal, vertical and shear stresses in fixed Cartesian system.
$\sigma_{\xi\xi}, \sigma_{zz}, \sigma_{z\xi}$	Horizontal, vertical and shear stresses in moving system.
σ_N, σ_T	Normal and tangential stresses on compaction front.
ω	Underrelaxation parameter for iterative analysis.
ω_0	Optimum value of ω .

SECTION I

INTRODUCTION

This paper presents a study of the problem of a progressing normal pressure on the surface of a layered half-space. The half-space consists of a single layer of a locking material that acts elastically after compaction and an underlying elastic material. The surface pressure moves with a constant velocity v , which is subseismic with respect to the speed of wave propagation in both the upper layer after compaction ($c_{p1} > c_{s1} > v$) and the underlying half-space ($c_{p2} > c_{s2} > v$). It is assumed that the load has been moving steadily for a long time so that a steady-state (of plane strain) exists with respect to a coordinate system attached to the moving load. The theory is developed for two types of progressing pressure loadings; (a) a case in which the progressing pressure is a step function in the coordinate $\xi = x + vt$ over a range of ξ very large, and then decays to zero at $\xi = \infty$, and (b) a case in which the progressing pressure has an exponential decay in the coordinate $\xi = x + vt$, Fig. 1.

It should be noted that the material description for the layer assumes a locking material that, after compaction, acts elastically. This mathematical model is an approximation

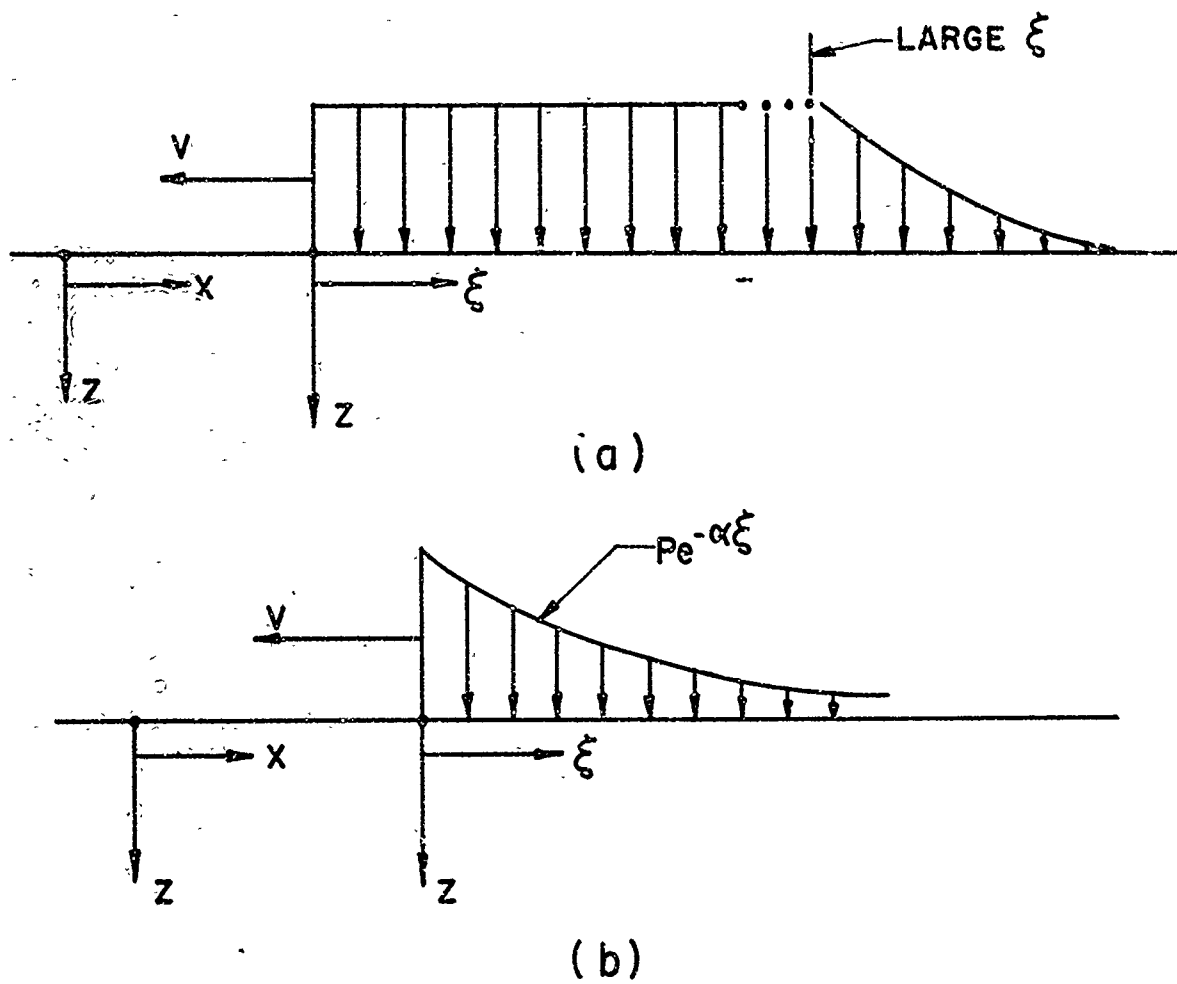


FIG. 1 - LOADING CONDITIONS

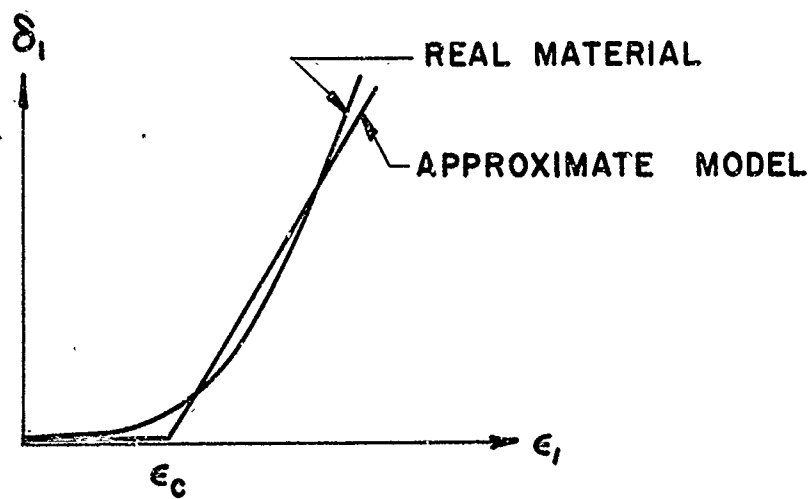


FIG. 2 - APPROXIMATION OF MATERIAL BY
LOCKING-ELASTIC MODEL

to certain types of real materials as shown in Fig. 2. The locking-elastic material has been previously studied by Bleich, Ref. [1].

In a previous paper, Ref. [2], the steady-state problem for a superseismic layer - subseismic half-space configuration was studied. For that case, the problem was of a mixed type, (a) hyperbolic in the superseismic layer and (b) elliptic in the underlying half-space. Consequently, signals from the underlying half-space outran the advancing surface pressure and the interaction stresses between the layers, i.e., σ_{zz} and $\sigma_{z\xi}$ extended over the entire plane $-\infty < \xi < \infty$. The entire layer and half-space were stressed, including that part of the region which was ahead of the moving load. Sharp shock fronts (P and S) were present in the superseismic layer, only behind the leading front of the moving load, Fig. 3.

The present problem differs from the one treated in Ref. [2] in a significant way, which is best understood by considering the layer to consist of a nonlinear hardening material, as indicated in Fig. 2. While the underlying half-space is subseismic in both the present case and in Ref. [2], the situation in the layer is superseismic at low stress levels, but subseismic at sufficiently high stress levels. In the present problem which considers the nonlinear material and a high stress level, there will, therefore, be a leading

shock corresponding to the first P-front in Fig. 3, but there will be no further shocks* to the right of (behind) this leading front. Ahead of this shock front, the stresses are inherently low. In the case of the locking material, Fig. 2, the shock corresponding to the first P-front in Fig. 3 is now identified with a compaction front, Fig. 4. The "low" stresses ahead of the front are assumed to vanish to permit the use of the locking concept. It will be further assumed that this compaction front is plane. This assumption is correct according to Ref. [1] in an infinite locking-elastic medium subjected to a progressing step wave, but not for a decaying pressure pulse where it is curved as indicated in Fig. 4. The curvature of this front is, however, not important if the layer thickness is not too large compared to the distance describing the decay of the applied surface pressure. The inclination of the locking front in the present analysis will be selected to be equal to the one found in Ref. [1] for a step pressure of intensity $P = P_0$. This leads to the configuration shown in Fig. 5. The problem becomes one of an irregularly shaped half-space with two layers, both of which are subseismic with respect to the moving velocity V , i.e., V is smaller than the velocity of dilatational (P) and equivoluminal (S) waves, in both layers. Hence, the differential equations of motion in both layers become elliptic

* There is a transition level at which the stress is insufficiently high and shear shock may occur. It is assumed in the present problem that the stress level is sufficiently high so that this does not occur.

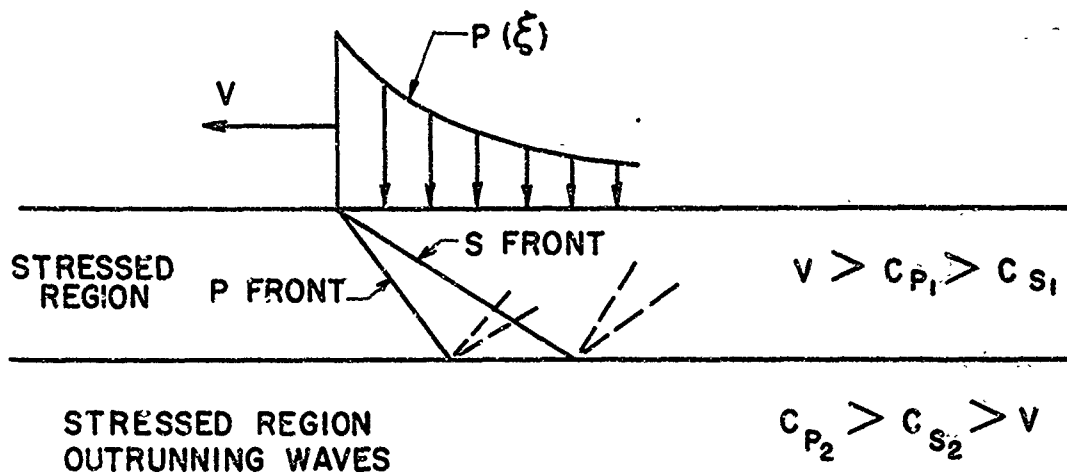


FIG. 3 - SUPERSEISMIC LAYER - SUBSEISMIC HALF SPACE
GEOMETRY OF REFERENCE [2]

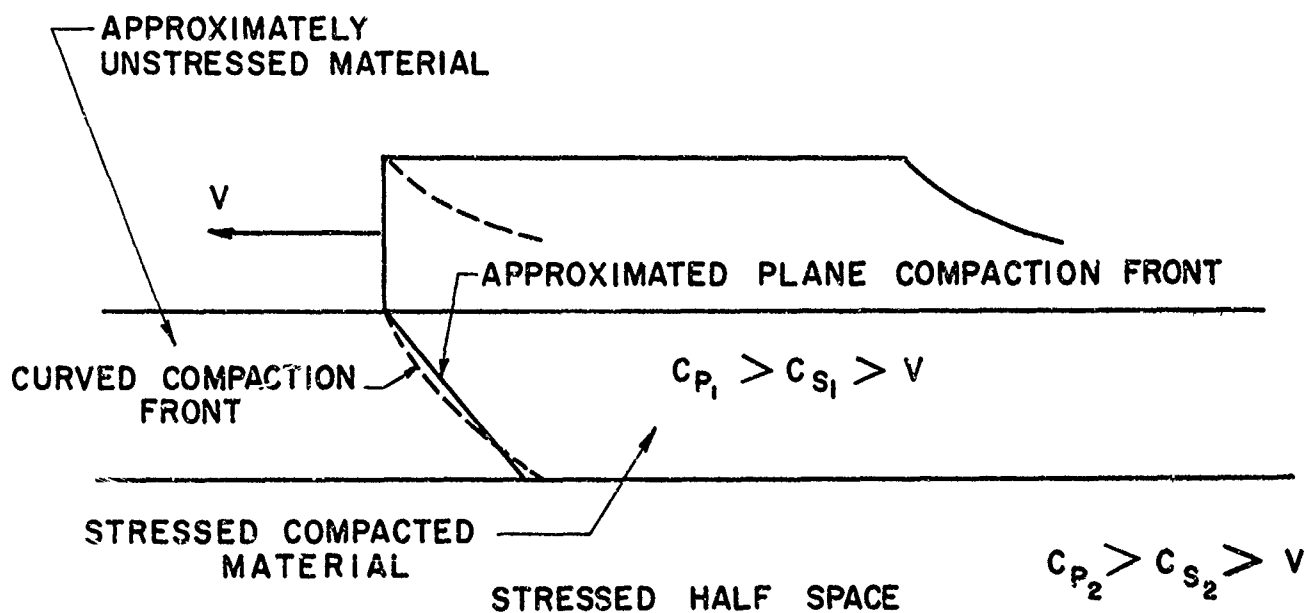


FIG. 4 - GEOMETRY OF PRESENT PROBLEM

and the solution reduces to that of an elliptical boundary value problem in the irregular domain of Fig. 5.

The elliptic nature of the problem leads to a system of simultaneous linear algebraic equations on the displacements at each point of a finite difference grid that covers the upper layer and the underlying half-space. A crucial approximate procedure, which is used in the numerical solution of the boundary value problem, should be discussed at this point. The actual domain of the boundary value problem discussed above extends to infinite in three directions, i.e., $-\infty < \xi < \infty$ and $0 \leq z < \infty$, Fig. 6. To obtain a finite number of algebraic simultaneous equations in the numerical analysis, the infinite domain is arbitrarily reduced to the finite domain ABCDEF as shown in Fig. 6, by assuming that the field quantities along the boundaries of the rectangle BFED are same as those that would be produced if a half-space of the underlying material was subjected to the same progressing pressure signal as in the actual problem, Fig. 7. Hence, it is assumed that the values of the field quantities along the boundary BCDEF of Fig. 6 will be those which occur in the same locations for the geometry of Fig. 7. These field quantities may be obtained by a direct integration of the Cole-Huth solution, Ref. [3]. In a similar manner, the field quantities on the line AB are approximated by values from the locking-elastic media study of Ref. [1] for the step pressure applied on an infinite half-

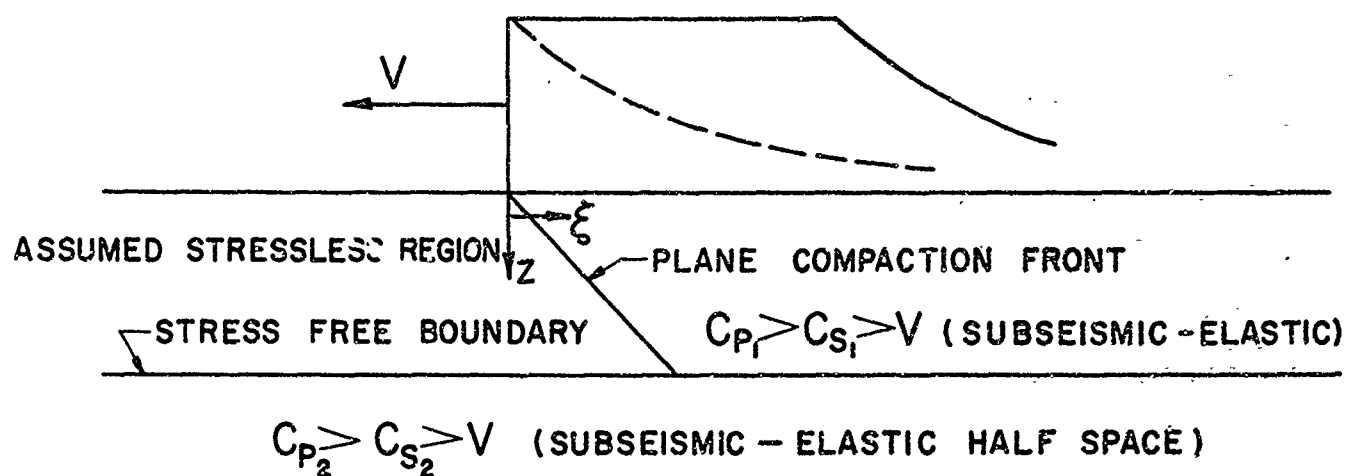


FIG. 5 - APPROXIMATE GEOMETRY FOR PRESENT PROBLEM

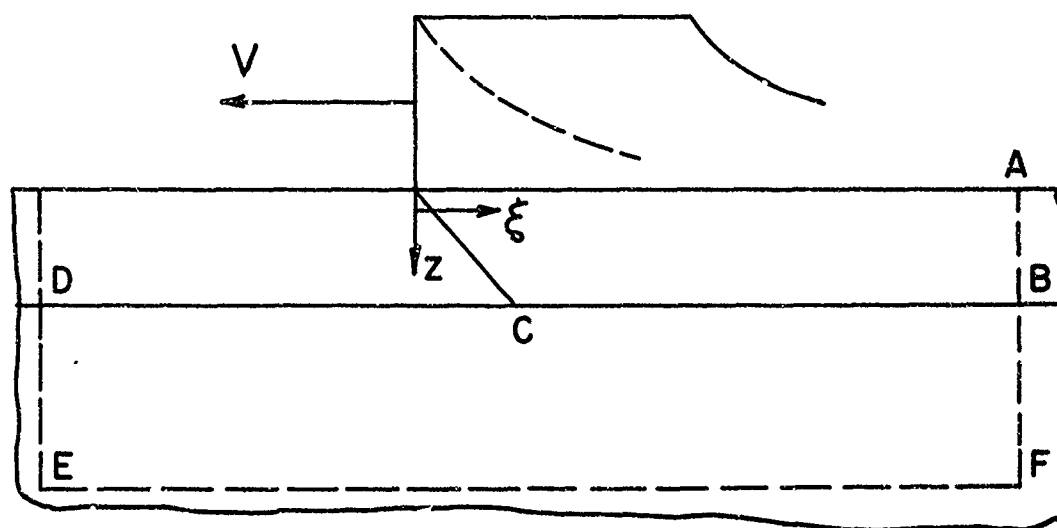


FIG. 6 -- BOUNDARY CONDITIONS AT LARGE $|\xi|$ AND z

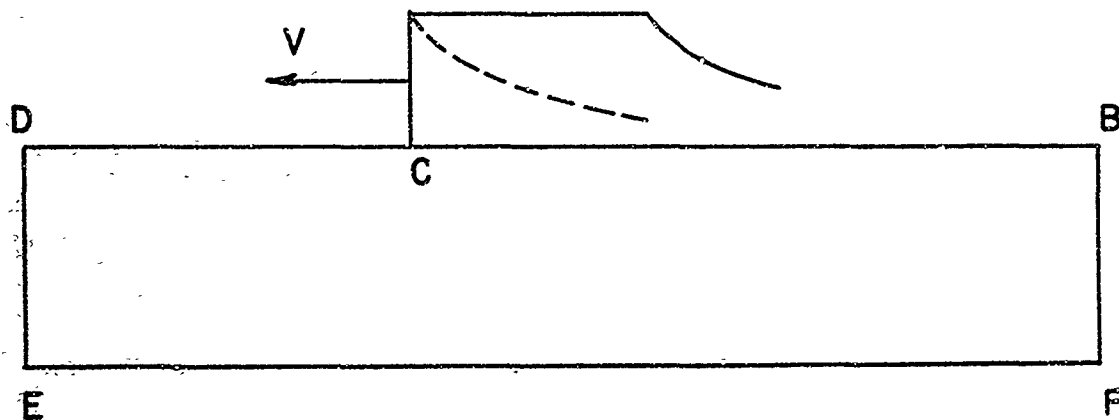


FIG. 7—BOUNDARY CONDITIONS IN HALF SPACE FOR LARGE $|\xi|$ AND z

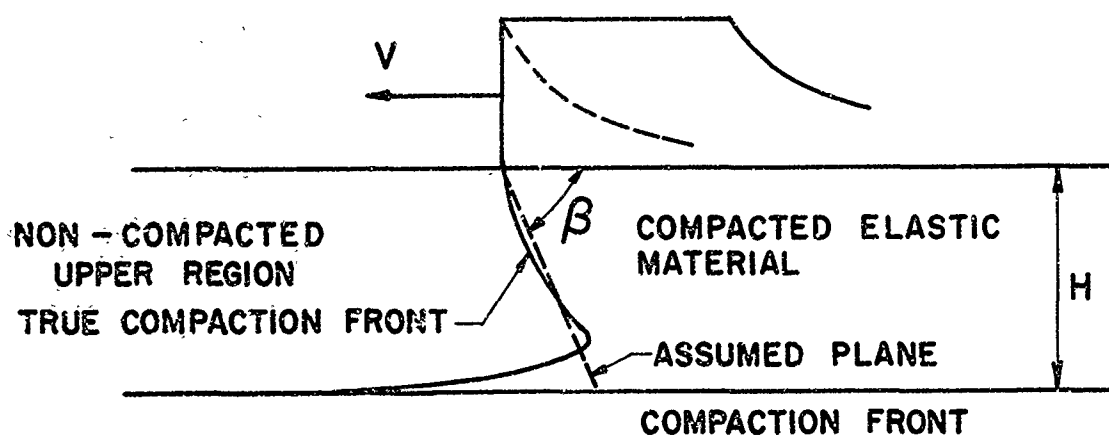


FIG. 8a—PLANE APPROXIMATION FOR COMPACTION FRONT IN LAYER

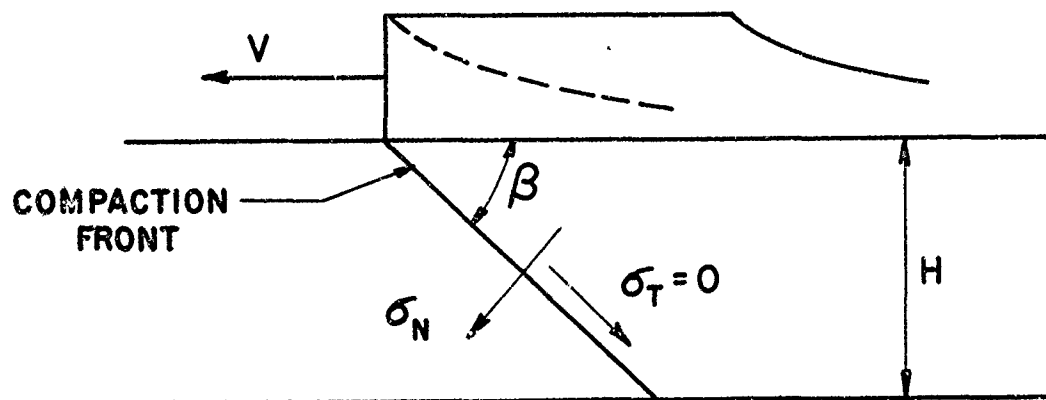


FIG. 8b—BOUNDARY CONDITIONS ON COMPACTION FRONT

space and by an integration of the Cole-Huth solution for a decaying pressure.

In defense of the approximation at the boundaries, it is noted that it is inherent that the stresses at far away boundaries do not effect the solution in the vicinity of the shock, i.e., the only region in which a steady-state solution has actual meaning. A computer code for the solution of the problem in the manner outlined has been developed and is available. Numerical results are shown for a typical configuration of interest.

Section II presents the equations for the basic formulation of the problem. The method of solution and some comments on the computer code are given in Section III. Finally, Section IV presents some numerical results and conclusions.

This paper is one of a series of steady-state solutions that have been obtained for various elastic and inelastic materials, Refs. [4]-[8]. While the solutions have been of interest in themselves, an additional purpose was to provide check results for several of the large finite difference and finite element computer codes, which are presently being used to study ground shock problems in elastic and inelastic media. Although these codes are primarily used for the solution of transient, rather than steady-state problems, they generally can also be used to model steady-state situations of the type considered here.

SECTION II

FORMULATION OF THE PROBLEM

Consider the geometry shown in Fig. 5 in which a layer of thickness H of a locking-elastic solid, overlies a half-space of a second elastic material. The layer is composed of a locking material, which, upon reaching a certain compacting strain ϵ_c , thereupon acts as a linear elastic homogeneous and isotropic material, Fig. 1. The surface $z = 0$ is subjected to a normal surface pressure which moves with a constant velocity V . The velocity V of the moving load is subseismic with respect to dilatational and equivoluminal wave velocities both in the compacted layer, i.e., $c_{p_1} > c_{s_1} > V$, and in the underlying half-space, $c_{p_2} > c_{s_2} > V$. A system of Cartesian coordinates is used in which z is normal to the layer surface and x is parallel to the surface in the direction of the moving load. The layer $0 \leq z \leq H$ is designated as region 1 and the half-space $z > H$ is designated as region 2. The corresponding elastic constants are indicated by the proper subscript.

For both the compacted elastic layer and the underlying half-space, the elastic stress-strain relations and the equations of motion for this plane strain problem are written as

$$\sigma_{xx} = \left(\frac{2G}{1-2\nu}\right) \left[(1-\nu) \frac{\partial u}{\partial x} + \nu \frac{\partial v}{\partial z} \right] \quad (1)$$

$$\sigma_{zz} = \left(\frac{2G}{1-2\nu}\right) \left[\nu \frac{\partial u}{\partial x} + (1-\nu) \frac{\partial v}{\partial z} \right] \quad (2)$$

$$\sigma_{xz} = G \left[\frac{\partial v}{\partial x} + \frac{\partial u}{\partial z} \right] \quad (3)$$

$$\frac{\partial \sigma_{xx}}{\partial x} + \frac{\partial \sigma_{xz}}{\partial z} = \rho \ddot{u} \quad (4)$$

$$\frac{\partial \sigma_{xz}}{\partial x} + \frac{\partial \sigma_{zz}}{\partial z} = \rho \ddot{v} \quad (5)$$

Eliminating the stresses between these equations, the displacement equations of motion become

$$(\lambda + 2\mu) \frac{\partial^2 u}{\partial x^2} + (\lambda + \mu) \frac{\partial^2 v}{\partial x \partial z} + \mu \frac{\partial^2 u}{\partial z^2} = \rho \frac{\partial^2 u}{\partial t^2} \quad (6)$$

$$(\lambda + 2\mu) \frac{\partial^2 v}{\partial z^2} + (\lambda + \mu) \frac{\partial^2 u}{\partial x \partial z} + \mu \frac{\partial^2 v}{\partial x^2} = \rho \frac{\partial^2 v}{\partial t^2} \quad (7)$$

For the steady-state problem under consideration a Galilean transformation $\xi = x + Vt$ is used to replace x and t by means of the relations

$$\frac{\partial}{\partial x} = \frac{\partial}{\partial \xi} \quad ; \quad \frac{\partial}{\partial t} = V \frac{\partial}{\partial \xi} \quad (8)$$

The stress-strain relations and the equations of motion become

$$\sigma_{xx} = \left(\frac{2G}{1-2\nu}\right) \left[(1-\nu) \frac{\partial u}{\partial \xi} + \nu \frac{\partial v}{\partial z} \right] \quad (9)$$

$$\sigma_{zz} = \left(\frac{2G}{1-2\nu}\right) \left[\nu \frac{\partial u}{\partial \xi} + (1-\nu) \frac{\partial v}{\partial z} \right] \quad (10)$$

$$\sigma_{xz} = G \left[\frac{\partial u}{\partial \xi} + \frac{\partial v}{\partial z} \right] \quad (11)$$

$$(\lambda + 2\mu - \rho v^2) \frac{\partial^2 u}{\partial \xi^2} + (\lambda + \mu) \frac{\partial^2 v}{\partial \xi \partial z} + \mu \frac{\partial^2 u}{\partial z^2} = 0 \quad (12)$$

$$(\lambda + 2\mu) \frac{\partial^2 v}{\partial z^2} + (\lambda + \mu) \frac{\partial^2 u}{\partial \xi \partial z} + (\mu - \rho v^2) \frac{\partial^2 v}{\partial \xi^2} = 0 \quad (13)$$

Note that

$$c_P^2 = \frac{\lambda + 2\mu}{\rho} \quad ; \quad c_S^2 = \frac{\mu}{\rho} \quad (14)$$

Equations (12) and (13) may be written in the form

$$A \frac{\partial^2 u}{\partial \xi^2} + B \frac{\partial^2 v}{\partial \xi \partial z} + C \frac{\partial^2 u}{\partial z^2} = 0 \quad (15)$$

$$D \frac{\partial^2 v}{\partial z^2} + E \frac{\partial^2 u}{\partial \xi \partial z} + F \frac{\partial^2 v}{\partial \xi^2} = 0 \quad (16)$$

where

$$\begin{aligned} A &= c_P^2 - v^2 & D &= c_P^2 \\ B &= c_P^2 - c_S^2 & E &= B \\ C &= c_S^2 & F &= c_S^2 - v^2 \end{aligned} \quad (17)$$

For the subseismic problem under consideration, the coefficients of Eqs. (17) are all positive and hence, the system of equations, Eqs. (15)-(16) are elliptic in nature. Consequently, the specified boundary conditions on the boundaries of the domain will uniquely determine the

solution of the equations of motion in the interior of the domain. The boundary conditions are developed below.

From Fig. 4, it is seen that boundary conditions must be specified on the surface $z=0$, on the compaction front of the locking-elastic layer, on the surface $z=H$ of the half-space ahead of the compaction front and on the layer half-space interface, $z=H$, behind the compaction front. The requirements on the stress and displacement quantities at $\xi = \infty$ and $z = \infty$ will be discussed in the section on the numerical computation of the displacements and stresses by means of a finite difference grid which is superimposed on the medium.

The boundary conditions on the surface $z=0$ are given by the relations

$$\sigma_{zz}(\xi, z=0) = -PU(\xi) \quad (18)$$

$$\sigma_{\xi z}(\xi, z=0) = 0 \quad (19)$$

while on the surface $z=H$ ahead of the compaction front (i.e., ξ negative)

$$\sigma_{zz}(\xi, z=H) = 0 \quad (20)$$

$$\sigma_{\xi z}(\xi, z=H) = 0 \quad (21)$$

The boundary conditions on the layer interface $z=H$ behind the compaction front require the continuity of stresses and displacements:

$$\left. \begin{aligned}
 u_1(\xi, z=H) &= u_2(\xi, z=H) \\
 v_1(\xi, z=H) &= v_2(\xi, z=H) \\
 \sigma_{zz,1}(\xi, z=H) &= \sigma_{zz,2}(\xi, z=H) \\
 \sigma_{\xi z,1}(\xi, z=H) &= \sigma_{\xi z,2}(\xi, z=H)
 \end{aligned} \right\} \quad (22)$$

The problem of a step load moving on the surface of a half-space of a locking material which upon compaction, becomes elastic and subseismic^{*)}, i.e., $c_{p2} > c_{s2} > V$, has been solved in Ref. [1]. It was shown that a stress discontinuity in the form of a compaction front occurs in the material and moves with the progressing surface pressure. For a step wave surface pressure loading, the compaction front will be plane, and the stress on the front will be normal to the front with no tangential component. The normal stress at the compaction front is given by the relation

$$\sigma_N = - \frac{(1-\nu)P}{\nu + (1-2\nu)\beta \cot \beta} \quad (23)$$

where β is the angle of the front with the surface $z=0$, Fig. 5a. The tangential stress on the compaction front is zero.

$$\sigma_T = 0 \quad (24)$$

*) The material after locking must have both its dilatational and equivoluminal velocities greater than the velocity V of the progressing load. This is a necessary condition for the continuity of the material behind the compaction front, i.e., a condition that prevents the locking front from separating from the material.

The angle of inclination β of the compaction front is given in terms of the velocity V of the moving surface pressure

$$V^2 = \frac{P}{\rho c} \frac{(1-v)}{v \sin^2 \beta + (1-2v) \sin \beta \cos \beta} \quad (25)$$

where

$$0 \leq \beta \leq \beta_{cr} \quad (26)$$

where the critical angle β_{cr} is defined by the relation

$$\frac{\tan(2\beta_{cr})}{\beta_{cr}} = -2(1-2v) \quad (27)$$

The fact that no steady-state solution is found if the velocity V is less than a critical value V_{cr} corresponding to β_{cr} is discussed in detail in Section III of Ref. [1] and will not be repeated here. It will be assumed that the β - V relation for the present problem is such that a steady-state solution exists and that the locking front meets the leading edge of the moving pressure loading at the point A in Fig. 5a.

As discussed in Section I of this paper, the compaction front for the present layered geometry is approximated by a plane front as shown in Fig. 5b. The boundary conditions on this front are given by the relations

$$\sigma_N(\xi, z) = - \frac{(1-v)P}{v + (1-2v)\beta \cot \beta} \quad (28)$$

$$\sigma_T(\xi, z) = 0 \quad (29)$$

where ξ and z are such that

$$\tan^{-1} \beta = -\frac{z}{\xi} \quad (30)$$

and the relation between β and V is given by Eq. (25).

The method of solution of this boundary value problem is discussed in Section III.

SECTION III

METHOD OF SOLUTION

The equations of motion, Eqs. (15)-(16) are integrated numerically at the pivotal points of a finite difference gridwork which is superimposed on the layer - underlying half-space geometry, Fig. 9. For the elliptic problem being solved, these differential equations are transformed into a set of simultaneous linear algebraic equations in the displacements u and v . As described in Section I, this infinite system of equations is truncated by applying approximate boundary conditions at all pivotal points which lie on the boundaries of a rectangle; these boundaries are located at a sufficiently large distance from the area of prime interest, i.e., the neighborhood of the compaction front in the layer and the shallow portions of the underlying half-space. Once the displacements are obtained, the stresses can be calculated at the corresponding grid points by means of finite difference operators.

The method of solution for the system of simultaneous algebraic equations was dictated by the available core size of the CDC 6600 computer that was utilized. An $M \times N$ gridwork of pivotal points leads to an unsymmetrical set of algebraic equations in $2MN$ unknowns. The band width of the equations are of the order of $4N$ and the core required for a standard type of inversion solution is of the order of $8MN^2$. For the large

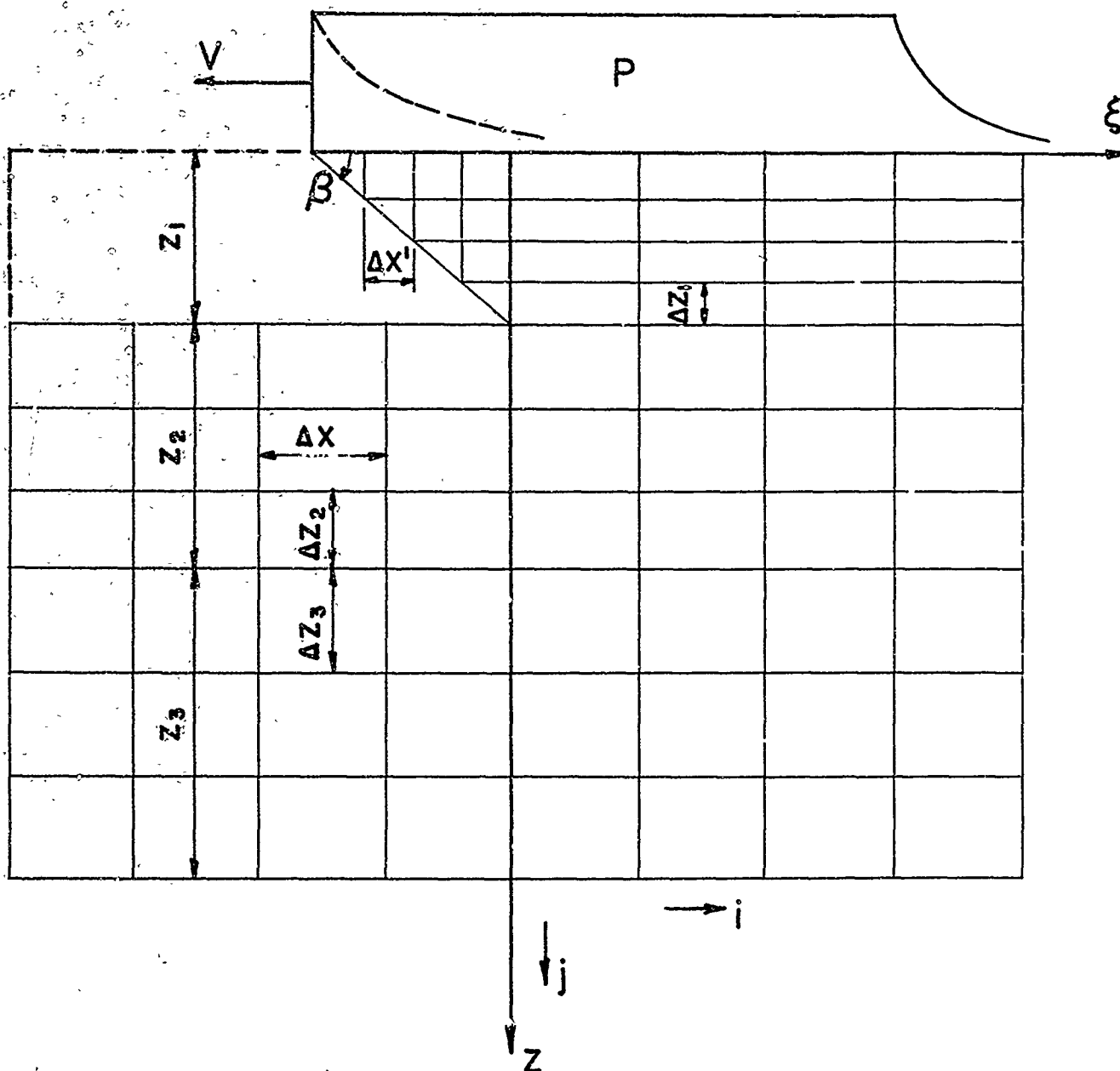


FIG.9 — FINITE DIFFERENCE GRID AND AXIS GEOMETRY
FOR NUMERICAL SOLUTION

number of points required to obtain acceptable detail in the present problem, the direct inversion approach became impracticable. Consequently, an alternative iterative technique was used in which the displacements u and v at each point in the $n+1$ approximation were calculated in terms of the corresponding values in the displacement field at the n^{th} approximation, as required by the appropriate finite difference operator at the pivotal point in question. In this iterative procedure, only $2MN$ of core was required and hence, this procedure was adopted.

A brief summary of the various finite difference equations which were utilized in the solution is presented in this section.

The partial differential equations, Eqs. (15)-(16) may be written at all ordinary interior pivotal points of the grid in terms of unequally spaced finite difference operators. Using the geometry of Fig. 10, the expressions for the various second derivative operators are given by

$$\left. \begin{aligned} D_{\xi} &= \frac{[i+1,j] - [i-1,j]}{h_{\ell} + h_r} \\ D_z &= \frac{[i,j+1] - [i,j-1]}{h_a + h_b} \end{aligned} \right\} \quad (31)$$

$$D_{\xi\xi}^2 = \frac{2}{h_r h_{\ell} (h_r + h_{\ell})} [h_r [i-1,j] - (h_r + h_{\ell}) [i,j] + h_{\ell} [i+1,j]] \quad (32)$$

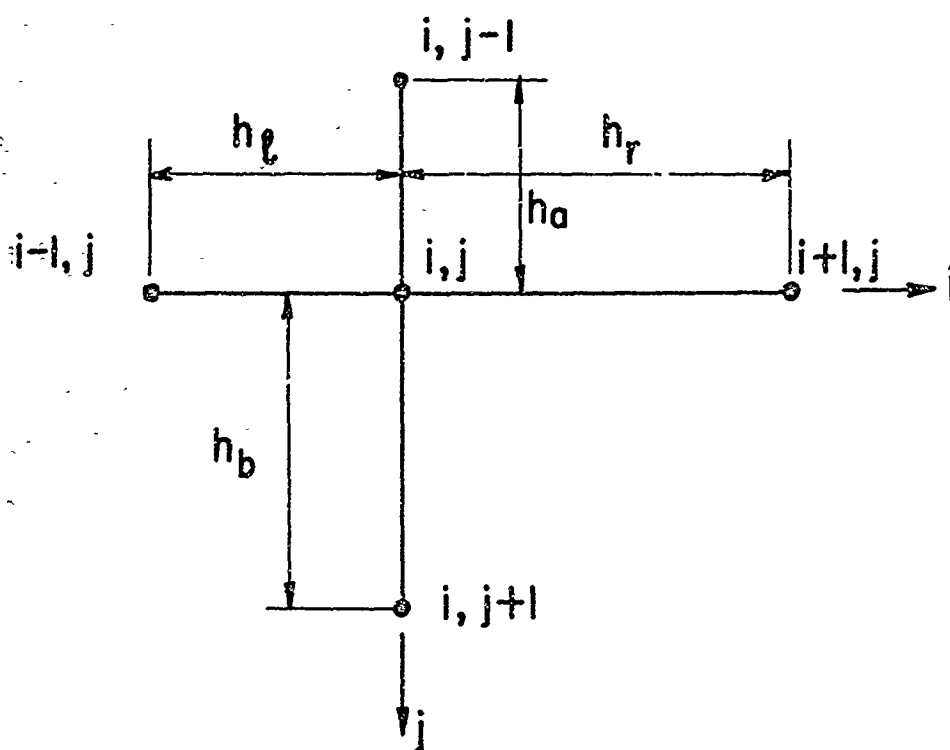


FIG. 10 — FINITE DIFFERENCE GRID

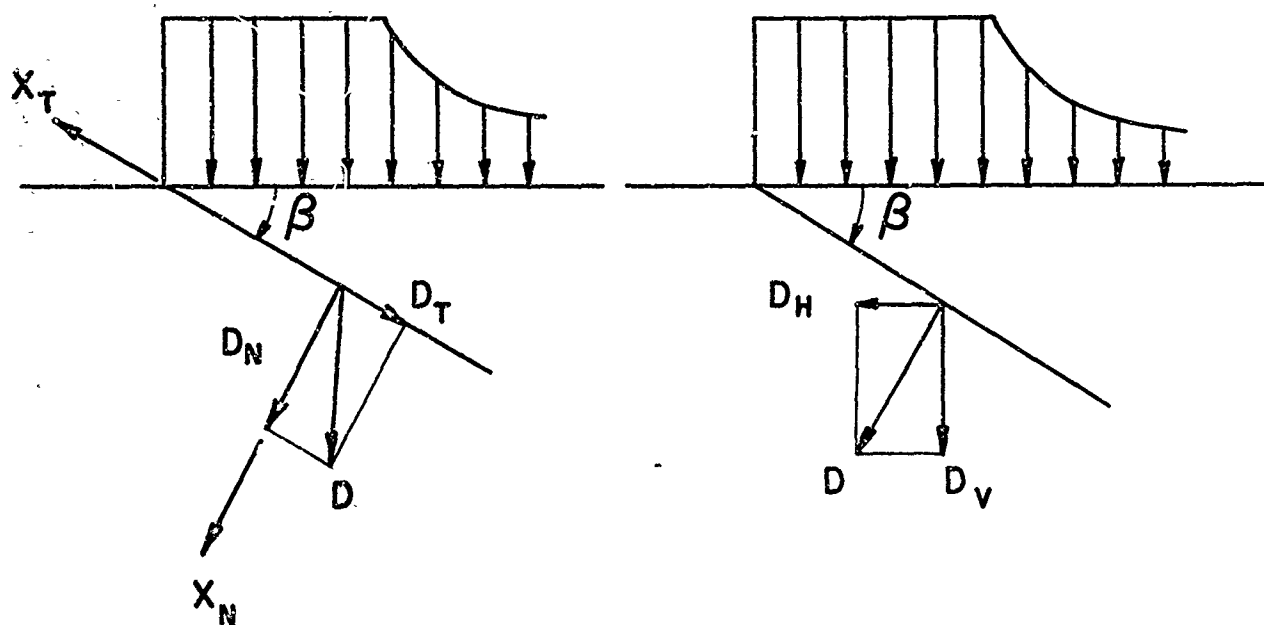


FIG. 11 — DISPLACEMENT RESOLUTION ON COMPACTION FRONT

$$D_{zz}^2 = \frac{2}{h_a h_b (h_a + h_b)} [h_b [i, j-1] - (h_a + h_b) [i, j] + h_a [i, j+1]] \quad (33)$$

$$D_{\xi z}^2 = \frac{1}{(h_\ell + h_r)(h_a + h_b)} [[i+1, j+1] - [i+1, j-1] - [i-1, j+1] + [i-1, j-1]] \quad (34)$$

Substituting Eqs. (31)-(34) into Eqs. (15)-(16) leads to a set of two simultaneous linear algebraic equations on the values of the displacements u and v :

$$\begin{aligned} & \frac{A}{h_\ell (h_r + h_\ell)} u_{i-1, j} - \frac{A}{h_r h_\ell} u_{i, j} + \frac{A}{h_r (h_r + h_\ell)} u_{i+1, j} + \\ & + \frac{B}{2(h_r + h_\ell)(h_a + h_b)} (v_{i+1, j+1} - v_{i+1, j-1} - v_{i-1, j+1} + v_{i-1, j-1}) + \\ & + \frac{C}{h_a (h_a + h_b)} u_{i, j-1} - \frac{C}{h_a h_b} u_{i, j} + \frac{C}{h_b (h_a + h_b)} u_{i, j+1} = 0 \end{aligned} \quad (35)$$

$$\begin{aligned} & \frac{F}{h_a (h_a + h_b)} v_{i, j-1} - \frac{F}{h_a h_b} v_{i, j} + \frac{F}{h_b (h_a + h_b)} v_{i, j+1} + \\ & + \frac{B}{2(h_a + h_b)(h_r + h_\ell)} [u_{i+1, j+1} - u_{i+1, j-1} - u_{i-1, j+1} + u_{i-1, j-1}] + \\ & + \frac{D}{h_\ell (h_r + h_\ell)} v_{i-1, j} - \frac{D}{h_r h_\ell} v_{i, j} + \frac{D}{h_r (h_r + h_\ell)} v_{i+1, j} = 0 \end{aligned} \quad (36)$$

Special formulas are of course required to express the various conditions at the boundaries of the problem. A brief description of the boundary conditions in finite difference form follows.

1. Boundary conditions at the compaction front

At the compaction front in the locking material layer, the normal stress is given by Eq. (23) and the tangential stress is set equal to zero. These conditions are written in terms of the displacement components and in the ξ, z system of coordinates. Writing the stress-displacement relations in the normal-tangential coordinate system, Fig. 11,

$$\sigma_N = \lambda \left[\frac{\partial u_N}{\partial x_N} + \frac{\partial u_T}{\partial x_T} \right] + 2\mu \frac{\partial u_N}{\partial x_N} \quad (37)$$

$$\sigma_T = \mu \left[\frac{\partial u_N}{\partial x_T} + \frac{\partial u_T}{\partial x_N} \right] \quad (38)$$

and using the $N, T - \xi, z$ transformation relations,

$$\left. \begin{aligned} u_N &= -u \sin \beta + v \cos \beta \\ u_T &= -u \cos \beta - v \sin \beta \\ \frac{\partial \xi}{\partial x_N} &= -\sin \beta & \frac{\partial \eta}{\partial x_N} &= \cos \beta \\ \frac{\partial \xi}{\partial x_T} &= -\cos \beta & \frac{\partial \eta}{\partial x_T} &= -\sin \beta \end{aligned} \right\} \quad (39)$$

the boundary conditions become

$$\left. \begin{aligned} (\lambda + \mu)P - (Q \cos 2\beta + R \sin 2\beta) &= \sigma_0 \\ Q \sin 2\beta - R \cos 2\beta &= 0 \end{aligned} \right\} \quad (40)$$

where

$$\left. \begin{aligned} P &= u_{\xi} + v_z \\ Q &= u_{\xi} - v_z \\ K &= u_z + v_{\xi} \end{aligned} \right\} \quad (41)$$

Simplifying Eqs. (40) to the form

$$\left. \begin{aligned} (\lambda + \mu)P - \frac{\mu}{\sin 2\beta} R &= \sigma_0 \\ Q \sin 2\beta - R \cos 2\beta &= 0 \end{aligned} \right\} \quad (42)$$

and substituting the finite difference operators of Eqs. (31) for the displacement derivatives in P, Q and R, Eqs. (42) can be solved for the displacements u and v, thus giving the boundary conditions for the pivotal points which lie on the compaction front.

2. Boundary conditions on the surface $z=0$ and on the interface $z=H$ (interface ahead of the shock front)

The boundary conditions on the surface $z=0$ are given by Eqs. (18)-(19). Using the finite difference operators of Eqs. (31), these conditions are written in terms of the boundary displacements as

$$u_{i,j} = u_{i,j+1} + K_2(v_{i+1,j} - v_{i-1,j}) \quad (43)$$

$$v_{i,j} = K_3(u_{i+1,j} - u_{i-1,j}) + v_{i,j+1} + K_5P \quad (44)$$

where

$$K_2 = \frac{h_b}{h_r + h_l}, \quad K_3 = \frac{K_2 \lambda}{\lambda + 2\mu}, \quad K_5 = \frac{h_b}{\lambda + 2\mu} \quad (45)$$

For the stress free surface $z=H$ which lies ahead of the compaction front, the quantity P is set equal to zero in Eqs. (43)-(44).

3. Continuity conditions on the interface behind the compaction front ($z=H, \xi > 0$)

The continuity conditions on this interface are given by Eqs. (22). The equations on the normal and tangential stresses at this interface are given in finite difference form by the relations

$$\begin{aligned} \left(\frac{\lambda_1 - \lambda_2}{h_l + h_r} \right) [u_{i+1,j} - u_{i-1,j}] + \left(\frac{\lambda_1 + 2\mu_1}{h_a} + \frac{\lambda_2 + 2\mu_2}{h_b} \right) v_{i,j} = \\ = \left(\frac{\lambda_2 + 2\mu_2}{h_b} \right) v_{i,j+1} + \left(\frac{\lambda_1 + 2\mu_1}{h_a} \right) v_{i,j-1} \end{aligned} \quad (46)$$

$$\begin{aligned} \left(\frac{\mu_1}{h_a} + \frac{\mu_2}{h_b} \right) u_{i,j} + \left(\frac{\mu_1 - \mu_2}{h_r + h_l} \right) [v_{i+1,j} - v_{i-1,j}] = \\ = \frac{\mu_1}{h_a} u_{i,j-1} + \frac{\mu_2}{h_b} u_{i,j+1} \end{aligned} \quad (47)$$

Equations (46)-(47) are solved for the displacements $u_{i,j}$ and $v_{i,j}$, thus giving the displacements on the surface $z=H$.

A special case occurs for the pivotal point which lies both on the compaction front and on the interface. At this point, one-sided forward differences must be used in the expression for the $\partial/\partial \xi$ operator and Eqs. (46)-(47) become:

$$\begin{aligned}
 -\frac{\lambda_1}{h_r} u_{i,j} + \left(\frac{\lambda_1 + 2\mu_1}{h_a} + \frac{\lambda_2 + 2\mu_2}{h_b} \right) v_{i,j} &= \left(\frac{\lambda_2}{h_l + h_r} - \frac{\lambda_1}{h_r} \right) u_{i+1,j} - \\
 -\frac{\lambda_2}{h_l + h_r} u_{i-1,j} + \left(\frac{\lambda_1 + 2\mu_1}{h_a} \right) v_{i,j-1} &+ \left(\frac{\lambda_2 + 2\mu_2}{h_b} \right) v_{i,j+1} \quad (48)
 \end{aligned}$$

$$\begin{aligned}
 \left(\frac{\mu_1}{h_a} + \frac{\mu_2}{h_b} \right) u_{i,j} - \frac{\mu_1}{h_r} v_{i,j} &= \frac{\mu_1}{h_a} u_{i,j-1} + \frac{\mu_2}{h_b} u_{i,j+1} + \\
 + \left(\frac{\mu_2}{h_l + h_r} - \frac{\mu_1}{h_r} \right) v_{i+1,j} &- \frac{\mu_2}{h_l + h_r} v_{i-1,j} \quad (49)
 \end{aligned}$$

Equations (48)-(49) may be solved for the displacements

$u_{i,j}$ and $v_{i,j}$ at the point in question

4. Special case for point which is both on the surface $z=0$ and the compaction front, Fig. 12

In order to express the requirement that the stress in the z -direction, σ_{zz} , at the point Q , (i,j) in Fig. 12 be equal to $-P$, it is necessary to define an operator for $\partial/\partial z$ at this point. This is done by utilizing a fictitious point M with coordinates $(i,j+1)$ and displacements u_M and v_M . The boundary conditions at the surface, Eqs. (18)-(19) are written in terms of the four unknown displacements $u_{i,j}$, $v_{i,j}$, u_M and v_M :

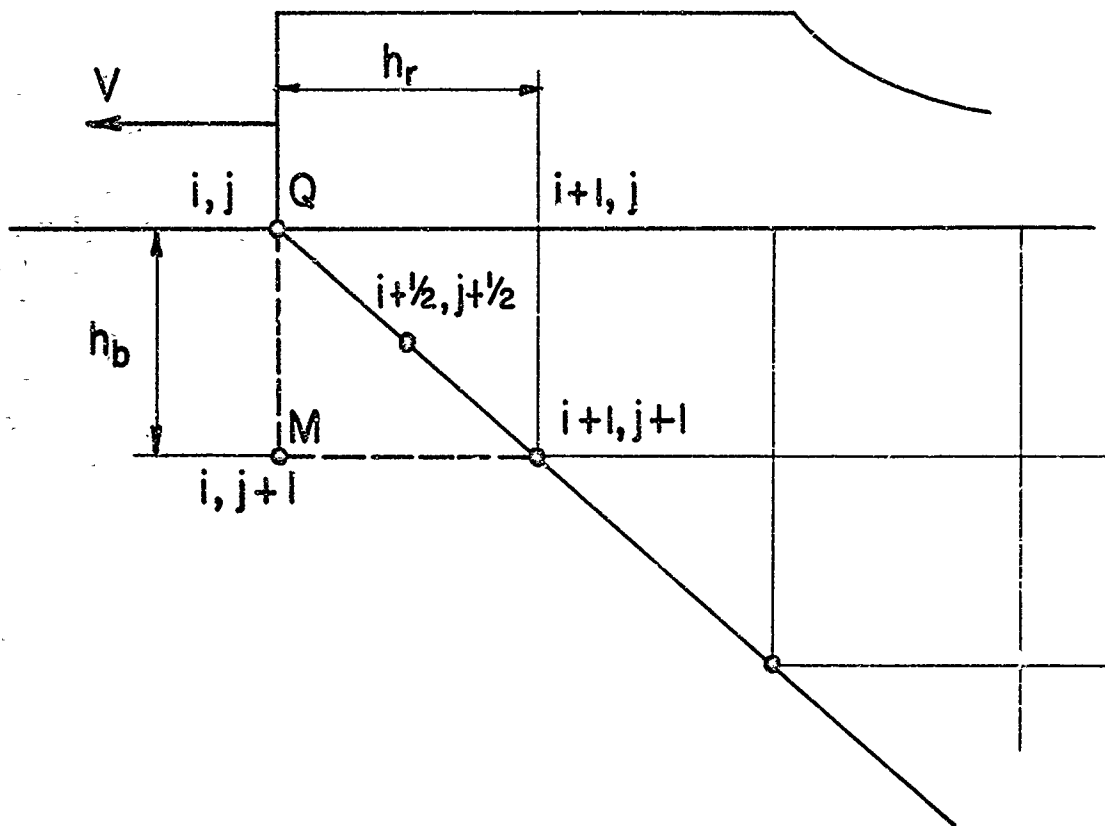


FIG. 12 — SPECIAL CASE FOR POINT Q

$$\sigma_{zz,ij} = \frac{\lambda_1}{h_r} [u_{i+1,j} - u_{i,j}] + \left(\frac{\lambda_1 + 2\mu_1}{h_b}\right) [v_M - v_{i,j}] = -P \quad (50)$$

$$\sigma_{zx,ij} = \frac{\mu_1}{h_b} [u_M - u_{i,j}] + \frac{\mu_1}{h_r} [v_{i+1,j} - v_{i,j}] = 0 \quad (51)$$

An additional two equations on these displacements are obtained from the boundary conditions on the normal and tangential stresses on the compaction front, Eqs. (42). These conditions are applied at the auxiliary point Q, $(i + \frac{1}{2}, j + \frac{1}{2})$ of Fig. 12 in terms of averages of the displacements at the surrounding points (i,j) , $(i+1,j)$, $(i+1,j+1)$ and $(i,j+1)$. The resulting equations are of the form of Eqs. (42) in which the quantities P, Q and R are given by

$$P = \frac{u_{i+1,j+1} + u_{i+1,j} - u_{i,j} - u_M}{2h_r} + \frac{v_M + v_{i+1,j+1} - v_{i,j} - v_{i+1,j}}{2h_b} \quad (52)$$

$$Q = \frac{u_{i+1,j+1} + u_{i+1,j} - u_{i,j} - u_M}{2h_r} - \frac{v_M + v_{i+1,j+1} - v_{i,j} - v_{i+1,j}}{2h_b} \quad (53)$$

$$R = \frac{u_M + u_{i+1,j+1} - u_{i,j} - u_{i+1,j}}{2h_b} + \frac{v_{i+1,j+1} + v_{i+1,j} - v_{i,j} - v_M}{2h_r} \quad (54)$$

Equations (42), (50) and (51) are solved for the four unknown displacements, thus giving the boundary values of the displacements u and v at this special point.

5. Approximate boundary conditions at large $|\xi|$ and z ,
Figures 6 and 7

In Section I, the method used to truncate the infinite set of finite difference equations on the displacements was described. Essentially, this was done by applying approximate boundary conditions at pivotal points on the boundaries of a rectangular domain BCDEF located at large distances ($|\xi|$ and z) from the domains of prime interest near the compaction front. These displacement quantities on the boundaries BCDEF of the subseismic half-space were obtained by direct integration on the computer of the corresponding quantities from the Cole-Huth solution for a point load P moving with subseismic velocity on the surface of a homogeneous isotropic elastic medium, Ref. [3]. The Cole-Huth displacements for the point load are given by Eqs. (25) and (26) of Ref. [3] and are repeated here for convenience:

$$u = P \frac{K_1}{\mu} \left(1 - \frac{\theta_L}{\pi}\right) - P \frac{\beta_T K_2}{\mu} \left(1 - \frac{\theta_T}{\pi}\right) \quad (55)$$

$$v = \frac{P}{\pi\mu} [K_2 \ln r_T - \beta_L K_1 \ln r_L] \quad (56)$$

where

$$K_1 = \frac{2 - M_T^2}{(2 - M_T^2)^2 - 4\beta_T\beta_L} \quad (57)$$

$$K_2 = \frac{2\beta_L}{(2 - M_T^2)^2 - 4\beta_T\beta_L} \quad (58)$$

$$\beta_L = (1 - M_L^2)^{1/2} \quad ; \quad \beta_T = (1 - M_T^2)^{1/2} \quad (59)$$

and

$$\left. \begin{aligned} \xi_L &= x + i\beta_L z = r_L e^{(i\theta_L)} \\ \xi_T &= x + i\beta_T z = r_T e^{(i\theta_T)} \\ 0 \leq \theta_L \quad ; \quad \theta_T \leq \pi \end{aligned} \right\} \quad (60)$$

The distributed loads of the present problem were resolved into a set of equivalent concentrated loads for the determination of these boundary conditions. A comprehensive study was made in order to assess the sensitivity of the displacements at pivotal points on the rectangular boundary BCDEF, on this resolution procedure. This involved a study of the influence in the half plane of the resolution of the distributed load into n concentrated loads of magnitude P/n spaced at a distance of Δx units apart. The results showed that the resolution of the distributed loads into n concentrated loads does not practically influence the displacements of points located at distances of 15 to 20 Δx from the central loading point, in the horizontal direction, and 20 to 25 Δx in the vertical direction. Hence, this concentrated load resolution approach was utilized for the present layered problem.

6. Iterative method for the solution of the system of linear algebraic equations using the over- and underrelaxation technique

The over- and underrelaxation iteration technique was utilized in the solution of the system of simultaneous algebraic equations on the displacements. This approach is described in detail in Ref. [9] and will be outlined in this section.

Assuming that the values of the displacement field at the $n-1$ and n^{th} cycles are known, a set of starting values for the $(n+1)$ cycle, u' , v' can be obtained by means of a linear interpolation (underrelaxation) of these previous values

$$\left. \begin{aligned} u' &= \omega u^{(n)} + (1-\omega) u^{(n-1)} \\ v' &= \omega v^{(n)} + (1-\omega) v^{(n-1)} \end{aligned} \right\} \omega < 1 \quad (61)$$

or a linear extrapolation with $\omega > 1$ (overrelaxation). The value of the parameter $\omega = 1$ would result in using $u^{(n)}$, $v^{(n)}$, the values of the displacement from the n^{th} iterative cycle as the starting values for the $n+1$ cycle. Using the values of u' and v' , Eqs. (61) as starting values, the values of $u^{(n+1)}$ and $v^{(n+1)}$ are obtained for the $n+1$ cycle.

From the theory of matrix iterative analysis, it may be shown that the relaxation factor ω should be chosen according to the following requirements:

- (1) There exists a limiting optimum value ω_0 for which the system converges most rapidly. If $\omega > \omega_0$, the

system converges, but with an oscillating pattern with respect to successive values of $u^{(n)}$ and $v^{(n)}$, a highly undesirable convergence for a digital computer since it can lead to unacceptable arithmetic conditions. Consequently, ω should be chosen to be smaller than this limiting value ω_0 .

- (2) The value of ω_0 depends on the grid size and decreases when the minimum spacing between two consecutive points is decreased.
- (3) For large grids in the present layered problem, ω_0 was found experimentally to be less than unity, thus requiring the use of underrelaxation, rather than overrelaxation.
- (4) The value of ω_0 varies as $u^{(n)}$ and $v^{(n)}$ approach their respective true values as the number of iterations n becomes large. It is therefore advantageous to use a variable $\omega^{(n)}$ in the calculations in order to speed the rate of convergence.

7. Finite difference stress - displacement relations

Once the displacements u and v have been obtained by the iteration, the stresses are computed using the stress-displacement relations in finite difference form:

$$\sigma_{\xi\xi} = (\lambda + 2\mu) \left[\frac{u_{i+1,j} - u_{i-1,j}}{h_r + h_\ell} \right] + \lambda \left[\frac{v_{i,j+1} - v_{i,j-1}}{h_a + h_b} \right] \quad (62)$$

$$\sigma_{zz} = \lambda \left[\frac{u_{i+1,j} - u_{i-1,j}}{h_r + h_\ell} \right] + (\lambda + 2\mu) \left[\frac{v_{i,j+1} - v_{i,j-1}}{h_a + h_b} \right] \quad (63)$$

$$\sigma_{\xi z} = \mu \left[\frac{u_{i,j+1} - u_{i,j-1}}{h_a + h_b} + \frac{v_{i+1,j} - v_{i-1,j}}{h_r + h_\ell} \right] \quad (64)$$

SECTION IV

NUMERICAL RESULTS AND DISCUSSION

This section presents a set of numerical results for the case of a progressing surface load with a step distribution in time. Results are presented for a typical configuration that has the following material and geometric constants:

$$c_{p_1} = 5,000 \text{ ft/sec}$$

$$v_1 = 0.25$$

$$\rho_1 = 2.85 \text{ lb sec}^2/\text{ft}^4$$

$$c_{p_2} = 8,000 \text{ ft/sec}$$

$$v_2 = 0.25$$

$$\rho_2 = 3.80 \text{ lb sec}^2/\text{ft}^4$$

$$H = 100 \text{ ft}$$

$$P_0 = 1 \text{ lb/ft}$$

$$V = 2,600 \text{ ft/sec}$$

It is of interest to consider the typical variation of the stresses σ_{zz} , $\sigma_{\xi z}$ and $\sigma_{\xi\xi}$ at points in both the layer and the half-space, Figs. 13-15 show the variation of these stresses with ξ at the depths $z = 60 \text{ ft}$ and $z = 80 \text{ ft}$ in the layer. It is seen that in each case, the stresses rise sharply behind the shock front, oscillate and then decay to

the following limits: $\sigma_{zz,L} = -P_0$, $\sigma_{z\xi,L} = 0$ and $\sigma_{\xi\xi,L} = 0$.

The peak value depends upon the velocity of the moving load and increases with increasing Mach numbers M_p and M_s . These stress amplifications are increased as the transonic case $M_s = 1$ is approached.

Figures 16-18 show the variation of the stresses σ_{zz} , $\sigma_{\xi z}$ and $\sigma_{\xi\xi}$ versus ξ at points in the underlying half-space at depth $z = 260$ ft and $z = 800$ ft. In this case, the peak values are located on a line that is inclined; the peak values for the deeper points occur for smaller values of ξ , i.e., they run ahead of the compaction front in the layer. Again, the peak values increase as M_p and M_s increase and approach high values as $M_s \rightarrow 1$, i.e., the sonic point is approached.

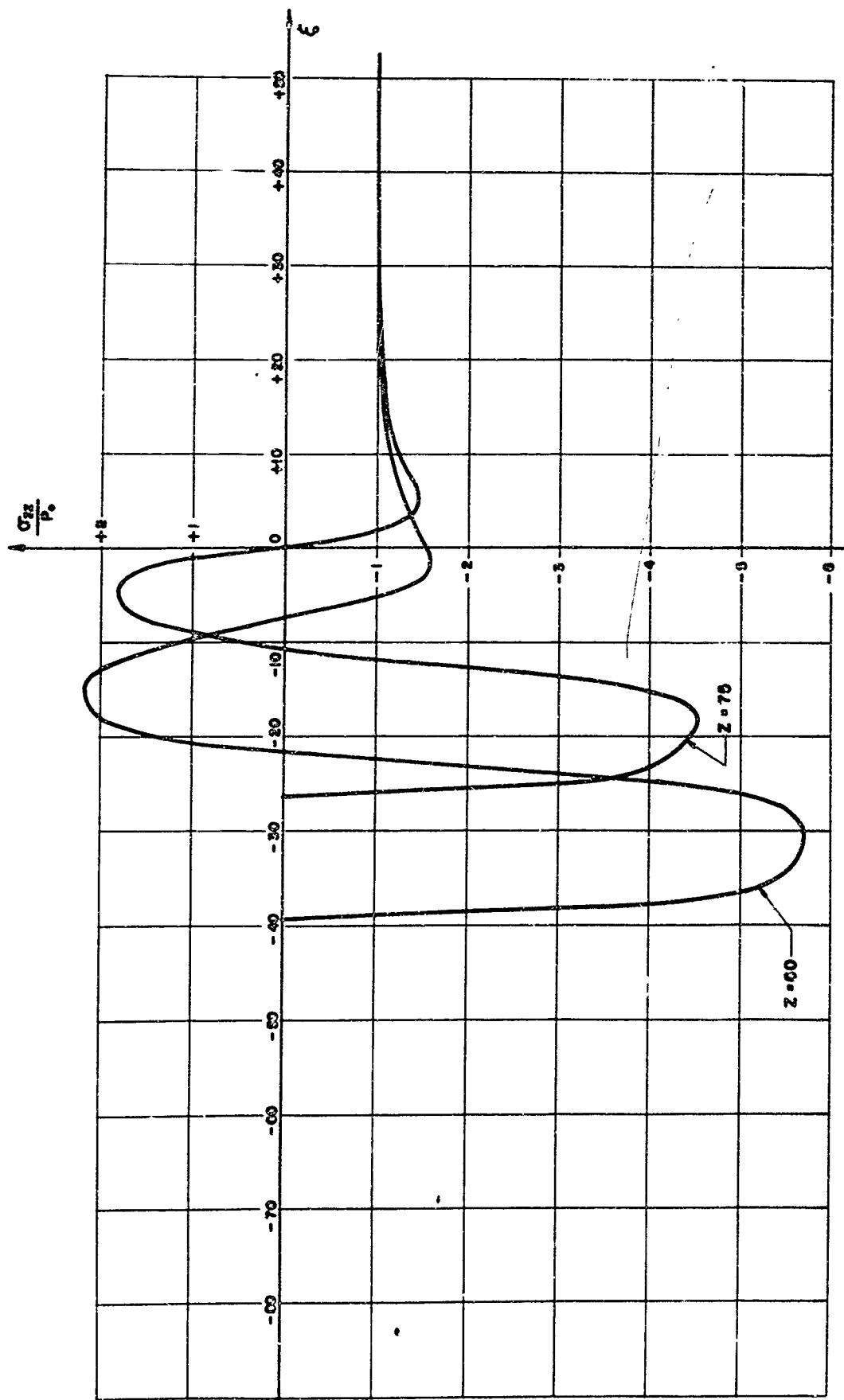


FIG. 13 - VERTICAL STRESS σ_{zz} vs. ξ IN UPPER LAYER

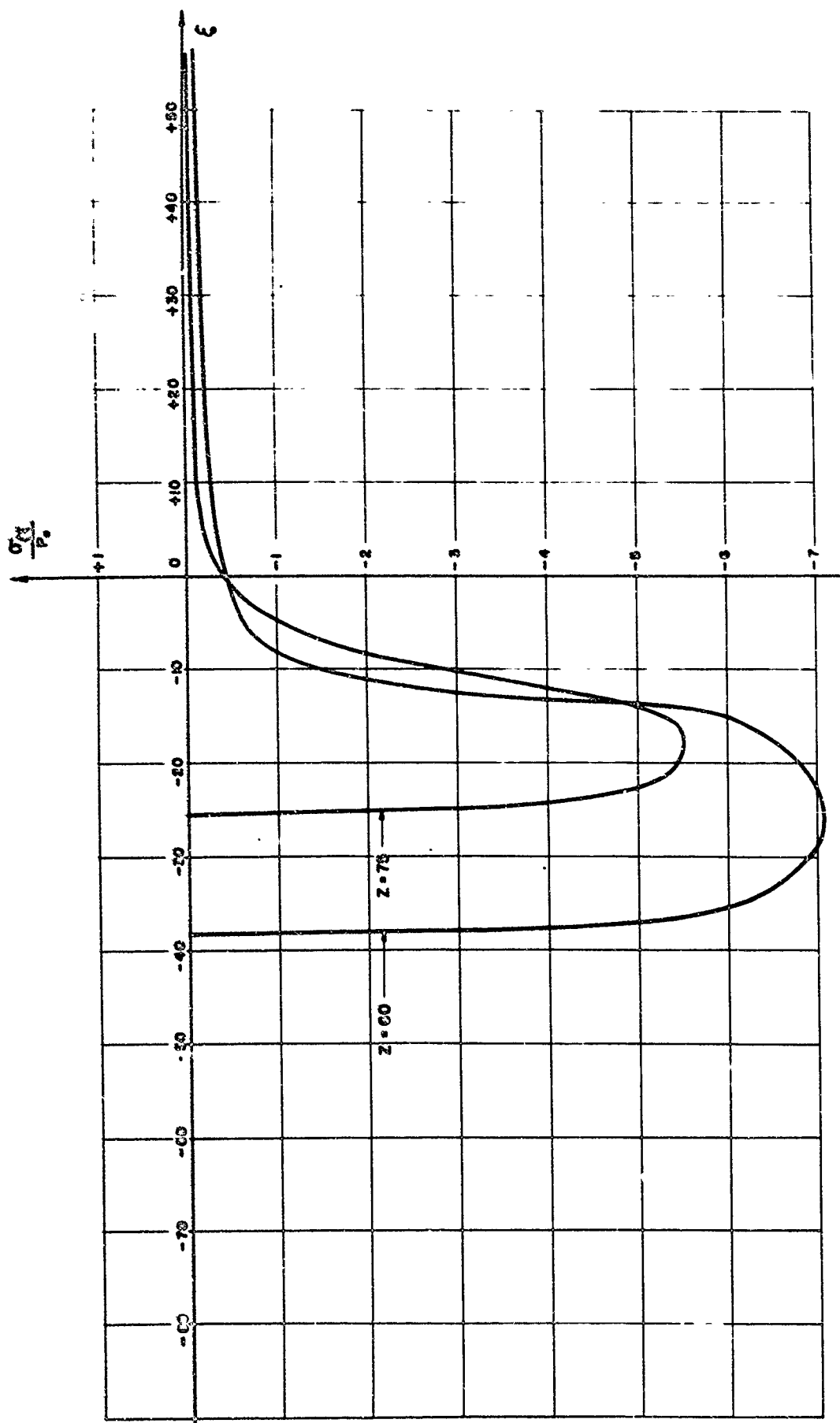


FIG. 14 - HORIZONTAL STRESS $\sigma_{\xi\xi}$ vs. ξ IN UPPER LAYER

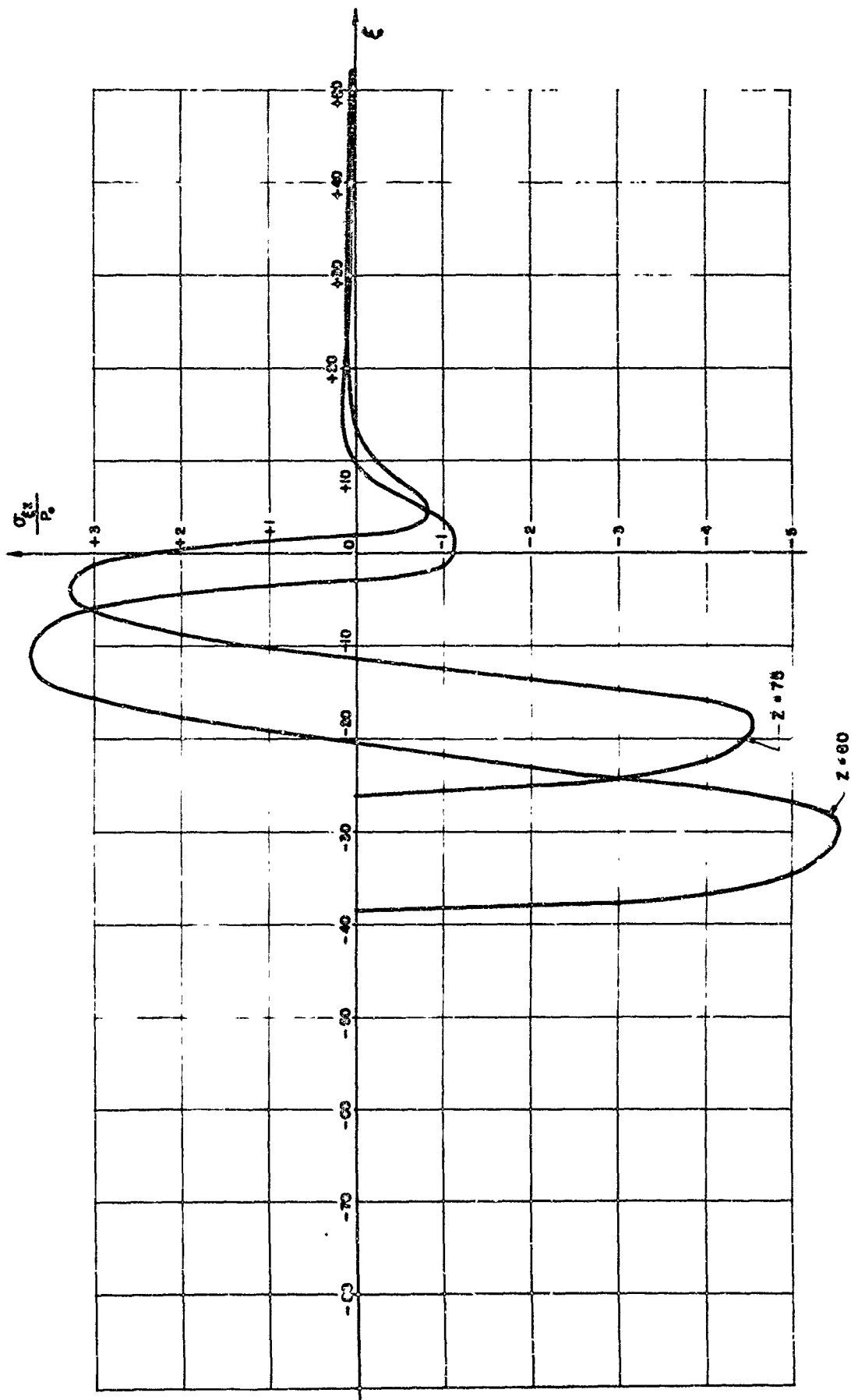


FIG. 15 -- SHEAR STRESS σ_{xz} vs z IN THE UPPER LAYER

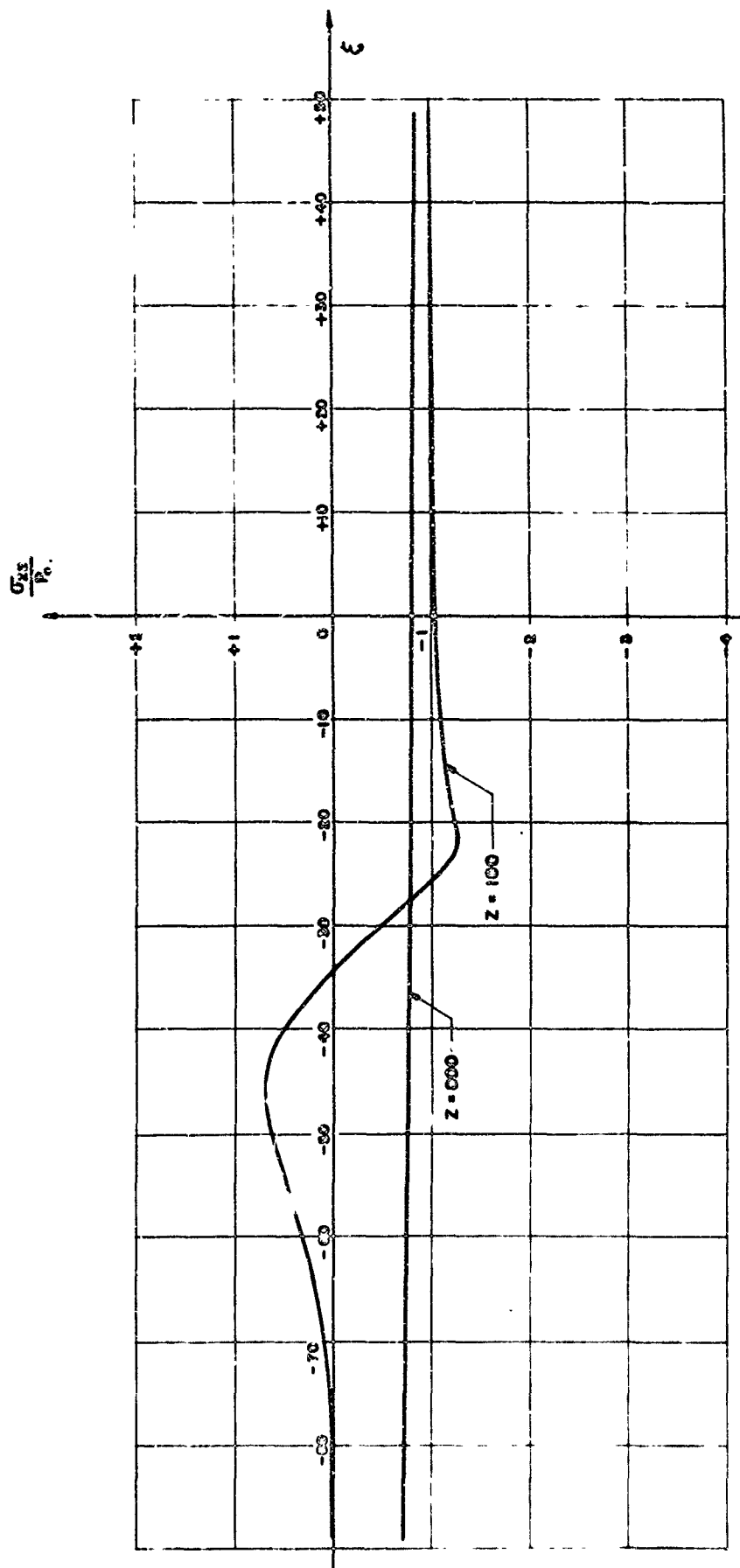


FIG. 16 -- VERTICAL STRESS σ_{zz} vs. ξ IN THE HALF-SPACE

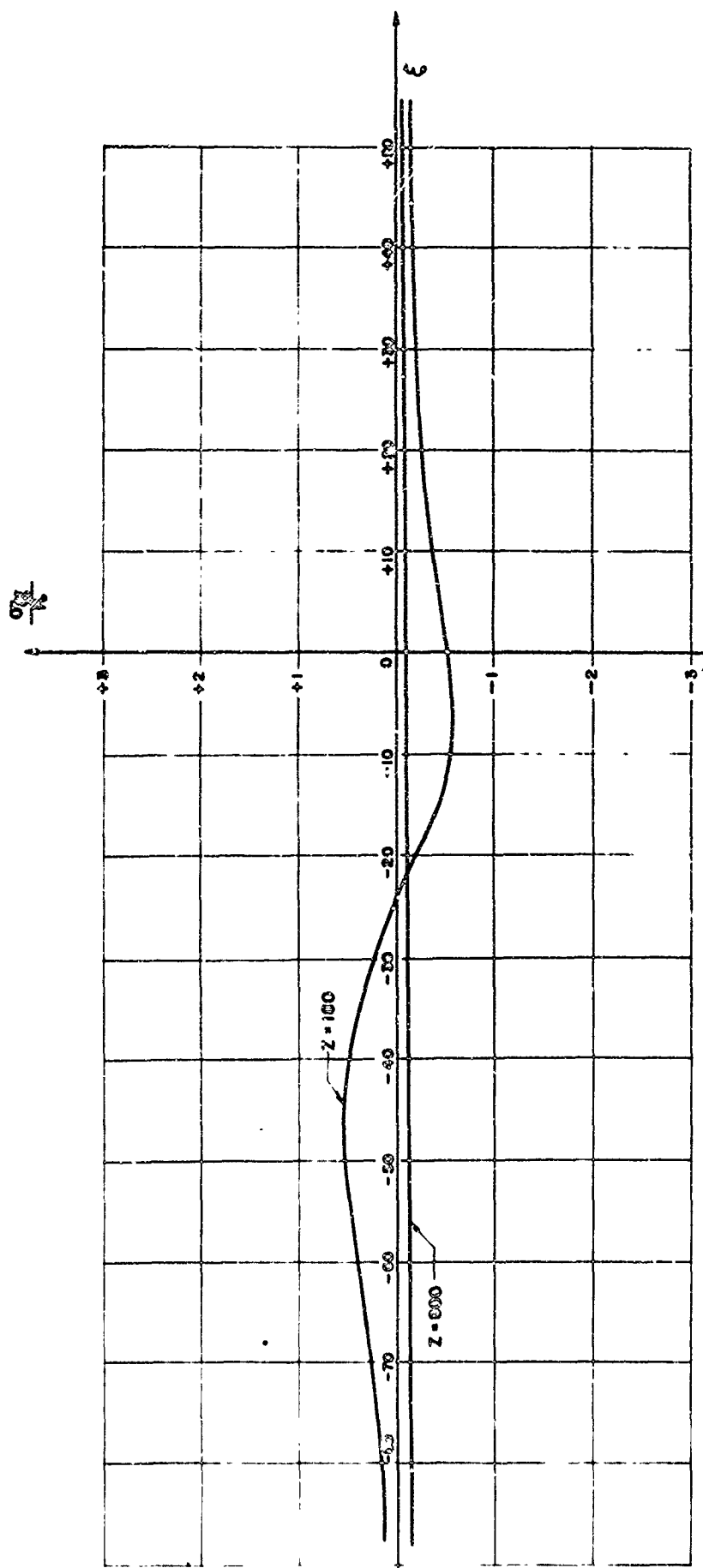


FIG. 17 - HORIZONTAL STRESS σ_{xx} vs. ξ IN THE HALF-SPACE

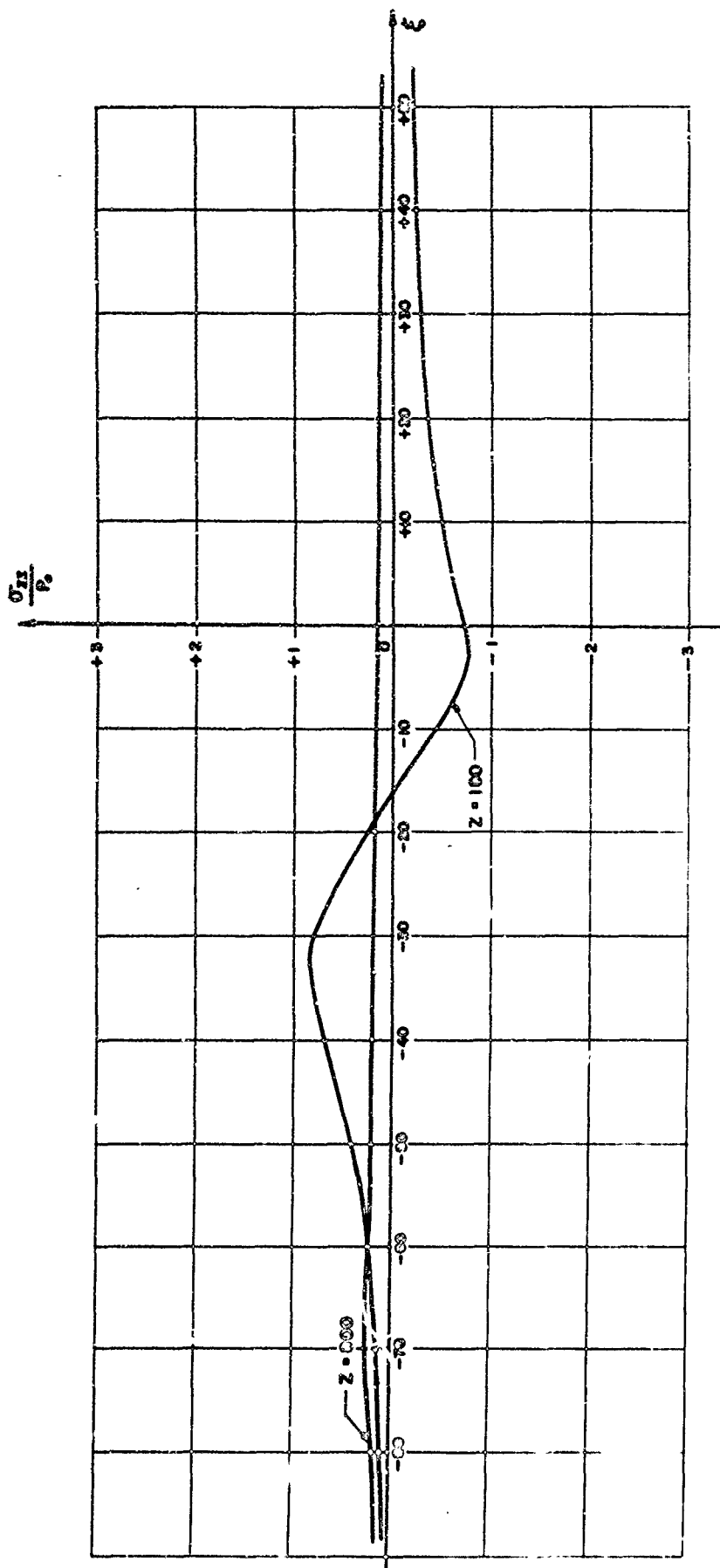


FIG. 10 — SHEAR STRESS σ_{xz} vs. ξ IN THE HALF-SPACE

REFERENCES

- [1] "Step Load Moving on the Surface of a Half-Space of a Locking Material - Subseismic Case", by H.H. Bleich, Technical Documentary Report No. WL-TDR-64-8, February 1965.

- [2] "Exponentially Decaying Pressure Pulse Moving with Constant Velocity on the Surface of a Layered Elastic Material - Superseismic Layer - Subseismic Half-Space", by Joseph P. Wright and Melvin L. Baron, Contract AF29(601)-7082, Technical Report No. AFWL-TR-67-136, June 1968.

- [3] "Stresses Produced in a Half-Plane by Moving Loads", by J. Cole and J. Huth, Journal of Applied Mechanics, Vol. 25, December 1958.

- [4] "Step Load Moving with Superseismic Velocity on the Surface of a Half-Space of Granular Material", by H.H. Bleich, A.T. Matthews and J.P. Wright, Technical Report AFWL-TR-65-59, Air Force Systems Command, Kirtland Air Force Base, September 1965.

- [5] "Stresses in an Elastic-Plastic Half-Space due to a Superseismic Step Load", by A.T. Matthews and H.H. Bleich, T.S.L., Ballistics Research Laboratory, Aberdeen Proving Grounds, Contract DA-30-069-AMC-8(R), Technical Report No. 4, March 1966.

- [6] "Step Load Moving with Superseismic Velocity on the Surface of an Elastic-Plastic Half-Space", by H.H. Bleich and A.T. Matthews, International Journal of Solids and Structures, Vol. 3, pp. 819-852, 1967.

- [7] "Exponentially Decaying Pressure Pulse Moving with Superseismic Velocity on the Surface of a Half-Space of a Granular Material", by H.H. Bleich and A.T. Matthews, Technical Report AFWL-TR-67-21, Contract AF29(601)-7082, July 1967.

- [8] "Exponentially Decaying Pressure Pulse Moving with Superseismic Velocity on the Surface of a Half-Space of a Von Mises Elastic-Plastic Material", by H.H. Bleich and A.T. Matthews, Technical Report No. AFWL-TR-68-46, Air Force Weapons Laboratory, May 1968.

- [9] "Matrix Iterative Analysis", by Richard S. Varga, Prentice-Hall, Chapter 3, 1962.

UNCLASSIFIED

Security Classification

DOCUMENT CONTROL DATA - R & D

(Security classification of title, body of abstract and indexing annotation must be entered when the overall report is classified)

1. ORIGINATING ACTIVITY (Corporate author) Paul Weidlinger & Associates 110 East 59th Street, 15th Floor New York, New York 10022		2a. REPORT SECURITY CLASSIFICATION UNCLASSIFIED	
3. REPORT TITLE PRESSURE PULSE MOVING WITH CONSTANT VELOCITY ON THE SURFACE OF A LAYERED MATERIAL [LOCKING-ELASTIC LAYER - SUBSEISMIC HALF-SPACE]		2b. GROUP	
4. DESCRIPTIVE NOTES (Type of report and inclusive dates) January 1968 to November 1968			
5. AUTHOR(S) (First name, middle initial, last name) Guy Bertrand Melvin L. Baron With the cooperation of Hans H. Bleich			
6. REPORT DATE May 1969		7a. TOTAL NO. OF PAGES 52	7b. NO. OF REFS 9
8a. CONTRACT OR GRANT NO. F29601-67-C-0091		8b. ORIGINATOR'S REPORT NUMBER(S) AFWL-TR-68-144	
b. PROJECT NO. 5710		9d. OTHER REPORT NO(S) (Any other numbers that may be assigned this report)	
c. Subtask: SB144			
10. DISTRIBUTION STATEMENT This document is subject to special export controls and each transmittal to foreign governments or foreign nationals may be made only with prior approval of AFWL (WLDC), Kirtland AFB, NM. Distribution is limited because of the technology discussed in the report.			
11. SUPPLEMENTARY NOTES		12. SPONSORING MILITARY ACTIVITY AFWL (WLDC) Kirtland AFB, NM 87117	
13. ABSTRACT (Distribution Limitation Statement No. 2) The response of a layered half-space to a progressing normal surface pressure is evaluated. The half-space consists of a single layer of a locking material that acts elastically after compaction, and an underlying elastic material. The surface pressure moves with a constant velocity V , which is subseismic with respect to the speed of wave propagation in both the upper layer after compaction and the underlying half-space. It is assumed that a steady-state exists with respect to a coordinate axis attached to the moving load. The essentially subseismic layer--subseismic half-space geometry leads to an elliptic problem that is solved by a finite difference iterative technique. A computer program for evaluating stresses and velocities at points in the medium is available and results are presented for a typical configuration of interest.			

DD FORM 1473

REPLACES DD FORM 1473, 1 JAN 64, WHICH IS OBSOLETE FOR ARMY USE.

UNCLASSIFIED

Security Classification

